Optimization of sensor design for Barkhausen noise measurement using finite element analysis

N. Prabhu Gaunkar, O. Kypris, I. C. Nlebedim, and D. C. Jiles

Citation: Journal of Applied Physics **115**, 17E512 (2014); doi: 10.1063/1.4864438
View online: http://dx.doi.org/10.1063/1.4864438
View Table of Contents: http://scitation.aip.org/content/aip/journal/jap/115/17?ver=pdfcov
Published by the AIP Publishing

Optimization of sensor design for Barkhausen noise measurement using finite element analysis

N. Prabhu Gaunkar,[a] O. Kypris, I. C. Nlebedim, and D. C. Jiles
Department of Electrical and Computer Engineering, Iowa State University, Ames, Iowa 50011, USA

(Presented 6 November 2013; received 24 September 2013; accepted 5 November 2013; published online 10 February 2014)

The effects of design parameters for optimizing the performance of sensors for magnetic Barkhausen emission measurement are presented. This study was performed using finite element analysis. The design parameters investigated include core material, core-tip curvature, core length, and pole spacing. Considering a combination of permeability and saturation magnetization, iron was selected as the core material among other materials investigated. Although a flat core-tip would result in higher magnetic flux concentration in the test specimen, a curved core-tip is preferred. The sensor-to-specimen coupling is thereby improved especially for materials with different surface geometries. Smaller pole spacing resulted in higher flux concentration. © *2014 AIP Publishing LLC*. [http://dx.doi.org/10.1063/1.4864438]

I. INTRODUCTION

Barkhausen emissions occur due to sudden changes in magnetization within a ferromagnetic material and are obtained with application of a continuously varying magnetic field.[1] The emissions can be measured as induced voltage signals using induction sensors. Due to the strong interrelationship between the magnetic properties and microstructural features in ferromagnetic materials, Barkhausen effect presents a powerful tool for non-destructively monitoring the condition of such materials. This can be done by correlating the peak amplitude of the voltage pulse obtained during Barkhausen emission measurement with stress.[2,3] For industrial equipment, such monitoring of structural health is essential to avoid failures resulting from micro-structural changes, residual stresses, surface deformations, and microcracks generated in operations.

Apart from the stress-state or other micro-structural inhomogeneities in the materials, the detected Barkhausen signal also depends on the magnetizing field produced by the coils, the core geometry, sensor-to-specimen coupling, and spacing between core tips. It is therefore important that the sensor configuration be optimized to improve the sensitivity, reproducibility, and accuracy of the detected Barkhausen signals. In this study, it is shown how the choice of sensor design parameters affects the generation of magnetic fields used to excite Barkhausen emissions in a specimen. Using finite element simulations a method of optimizing these parameters for sensors with C-core geometries with two windings is demonstrated. The choice of performing DC simulations and thus ignoring frequency dependent effects is supported by the fact that typical Barkhausen noise excitation coils operate in the lower quasi-static limit and are thus well described by a DC approach.

II. THEORY

From Ampere's circuital law, for a magnetic circuit

$$\oint \mathbf{H} \cdot d\ell = NI. \tag{1}$$

Here **H** is the magnetic field strength in the core, generated due to current I flowing in a coil having N turns. ℓ is the length of the flux path. The equivalent circuit of the magnetizing unit for this study is shown in Fig. 1(a). The total magnetic field strength due to the two magnetizing coils is taken to be 0.5 kA/m, in line with a previous study[4] on Barkhausen measurement. The two magnetizing coils can be approximated as solenoids of finite lengths. We can therefore find the field intensity along the axis, at a distance x from the center of the solenoid using the relation[5,6]

$$H = \frac{NI}{L}\left(\frac{L+2x}{2\sqrt{D^2+(L+2x)^2}} + \frac{L-2x}{2\sqrt{D^2+(L-2x)^2}}\right). \tag{2}$$

D is the coil diameter, which for a C-core represents a coil with value shown in Table I. L is the length of the magnetizing coil. The magnetic field at the off-axis point C, which in this study is the center of the test specimen, is considered to be equivalent to the on-axis field at a distance x from the center of the coil. This is a valid approximation since the magnetic flux path is curved by the material, thus making it possible to set x = ABC. Therefore, we use this relationship to approximate the value of the magnetic field at the point marked C. Since the analytical expression is an approximation of the magnetic field at point C, we utilized finite element simulations for improved accuracy.

III. SIMULATION

Fig. 1(b) shows the geometry of the magnetizing unit. C-core geometry was selected, being a typical geometry for Barkhausen sensors. The number of turns and coil length for the magnetizing coils were calculated using Eq. (2). A DC magnetizing current of 1 A was assumed. The properties and dimensions of the core and the coil are listed in Table I. A finite element simulation was performed using the AC/DC module of COMSOL Multiphysics.

[a]Author to whom correspondence should be addressed. Electronic mail: neelampg@iastate.edu.

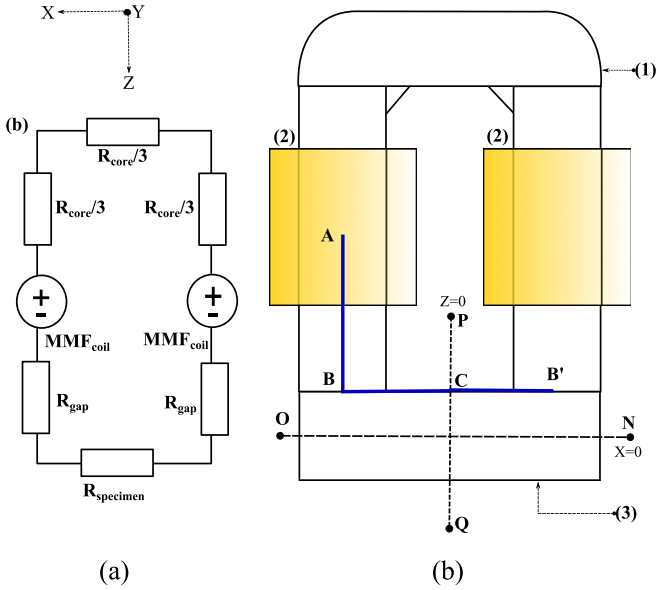

FIG. 1. (a) The equivalent magnetic circuit. (b) Schematic of the magnetizing assembly showing the core material (1), coils (2), and test specimen (3). Line segments NO and PQ represent sections along X and Z direction, respectively.

IV. RESULTS AND DISCUSSION

The effects of using different core materials for the magnetizing unit and the variations in the tip-curvature, length and inter-pole spacing of the core-materials have been investigated.

A. Effect of core material

Table II shows the core materials investigated including their electrical and magnetic properties. It can be seen in Fig. 2 that the maximum magnetic flux density in the material corresponds to the material with highest permeability. Although permalloy has the highest flux concentration, its saturation magnetization (0.86×10^6 A/m) is almost half of that of iron (1.71×10^6 A/m). Since it is important not to saturate the core material in application, iron was selected as the choice material for the rest of the study.

TABLE I. Core and coil dimensions (per pole).

Sensor	Coil	Core
Material	Copper	Variable
Length	8 mm	14 mm
Width	4 mm	3.4 mm
Depth	4 mm	3.4 mm
Number of Turns	32	N/A

TABLE II. Properties of the materials studied for use as the core material of the magnetizing unit.

Material	Electrical Conductivity S/m	Relative Permeability	Relative Permittivity
Air	0	1	1
Iron	1E7	5000 (Ref. 7)	300 (Ref. 8)
78 Permalloy	0.5E7	100000	5000 (Ref. 8)
Electrical Steel	2.12E6	4000	1
Ni-Zn Ferrite	2E-5 (Ref. 9)	1000 (Ref. 10)	14 (Ref. 9)

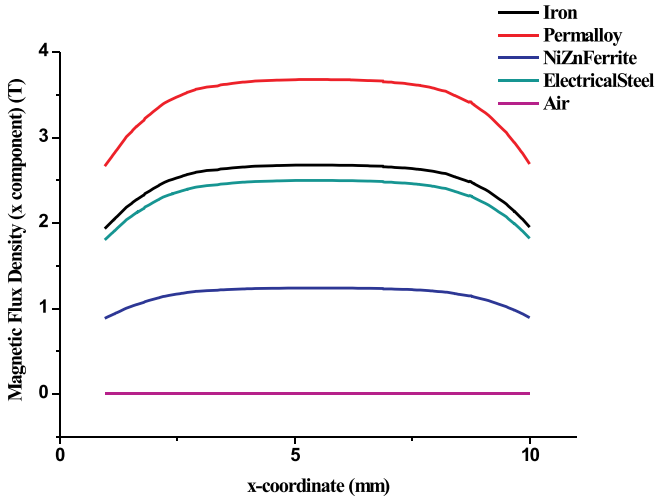

FIG. 2. Effect of material on magnetic flux density. Magnetic flux density was measured between the pole centers along the line segment NO as seen in Fig. 1(b).

B. Effect of core-tip curvature

The effect of core-tip curvature on the magnetic flux density in the sample is shown in Fig. 3. The curvature of the core-tip is an important parameter to ensure good sensor-to-specimen coupling. Cores with flat, pointed and curved tips were investigated. Fig. 3 shows that the best performance can be obtained using a core-material with a flat tip. Nevertheless, in applications, a curved core-tip helps ensure consistent flux coupling with test specimens of varying surface geometries. Hence the core-tip curvature selected has an arc length of 3.45 mm that is slightly more than the length of a flat tip. Magnetic flux leakage occurs in the region between the core poles resulting in asymmetrical flux density above and below the test specimen.

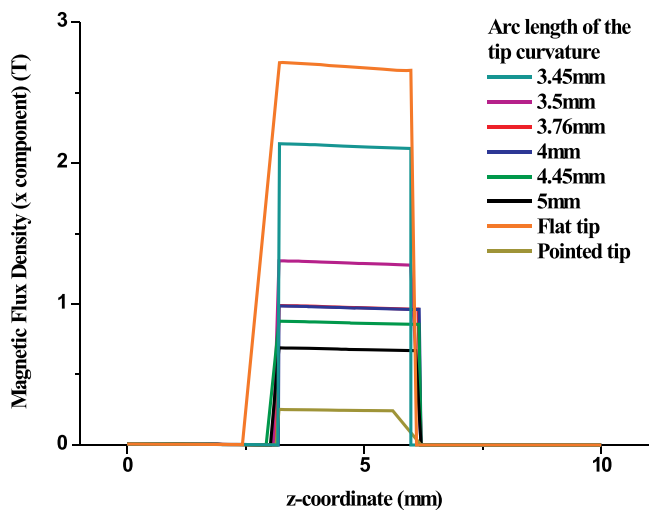

FIG. 3. Effect of tip curvature on the magnetic flux density. Magnetic flux density was measured along the line segment PQ as shown in Fig. 1(b).

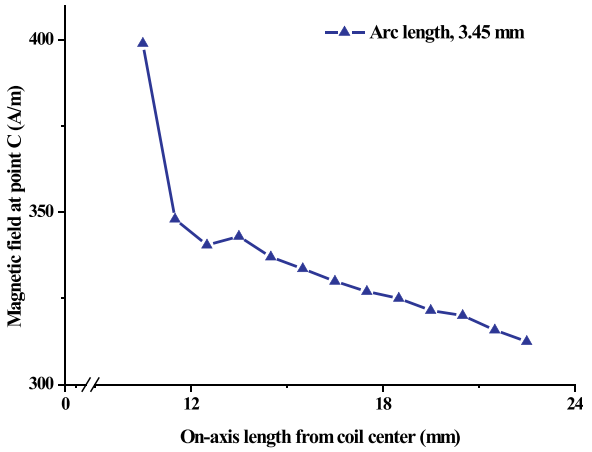

FIG. 4. Effect of core length on magnetic field. The on-axis length from coil center is defined as the length along path ABC, shown in Fig. 1(b). AB varies with increasing length of poles.

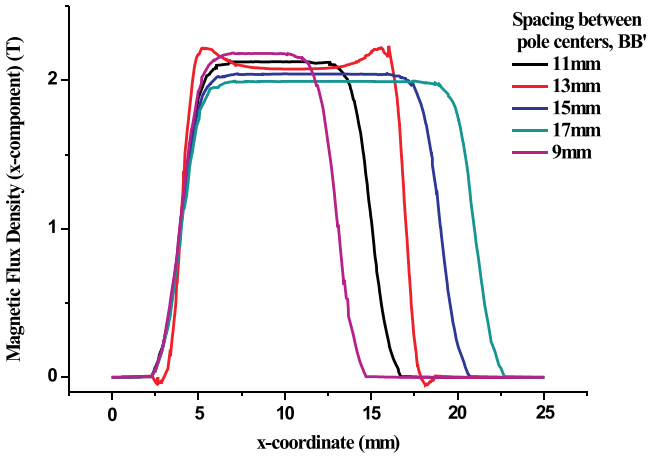

FIG. 5. Effect of pole spacing. The pole spacing was measured along the line segment NO, as shown in Fig. 1(b), where BB′ indicates the spacing between the pole centers.

C. Effect of core length

The effect of path length, ABC, of the core material on the generated magnetic field is shown in Fig. 4. These are obtained using an iron core with an arc length of 3.45 mm. The magnetic field strength decreases with increasing length of the core material. This is an important design consideration especially where varying the sensor size is necessary to test different parts of the same component. The maximum field strengths obtained at point C are in the range 0.31–0.4 kA/m. This is less than the 0.5 kA/m calculated and might be due to flux leakage. The maximum field penetration is obtained with the magnetizing coils are placed at a distance of 0.5 mm (i.e., closest to the test specimen). This was incorporated into the design to observe the effect of spacing between the poles of the sensor.

D. Effect of inter-pole spacing

Fig. 5 shows the effect of varying the spacing between the two poles of the sensor. It can be seen that small spacing maximizes the magnetic flux density. In application, however, maximizing the flux density by decreasing the pole spacing should be balanced with the fact that measurement noise increases due to mutual inductance when the pole spacing is reduced. This is important considering that Barkhausen emissions are already noise-like.

V. CONCLUSIONS

The study carried out on the optimization of the sensor design parameters for Barkhausen emission measurements revealed the following. A sensor constructed with soft iron resulted in high magnetic field penetration into the test specimen. The sensor geometry governed the coupling between the sensor and the test specimen, a flat tip resulting in the best coupling. The sensor design can be further optimized to suit specific applications taking into consideration the parameters analyzed and described in this study.

ACKNOWLEDGMENTS

This research was funded by the Department of Electrical and Computer Engineering, Iowa State University and the ASNT Fellowship Award.

[1]A. Dhar and D. Atherton, IEEE Trans. Magn. **28**, 3363 (1992).
[2]O. Kypris, I. C. Nlebedim, and D. C. Jiles, IEEE Trans. Magn. **48**, 4428 (2012).
[3]L. Mierczak, D. C. Jiles, and G. Fantoni, IEEE Trans. Magn. **47**, 459 (2011).
[4]O. Kypris, I. C. Nlebedim, and D. C. Jiles, IEEE Trans. Magn. **49**, 4148 (2013).
[5]D. C. Jiles, *Introduction to Magnetism and Magnetic Materials*, 1st ed. (Chapman and Hall, London and New York, 1991).
[6]A. E. Umenei, Y. Melikhov, and D. C. Jiles, IEEE Trans. Magn. **47**, 734 (2011).
[7]D. D. L. Chung, *Functional Materials: Electrical, Dielectric, Electromagnetic, Optical and Magnetic Applications (with Companion Solution Manual)*, Engineering Materials for Technological Needs Vol. 2 (World Scientific, Hackensack and New Jersey, London, 2010).
[8]J. S. Wilson, *Sensor Technology Handbook* (Elsevier, Amsterdam and Boston, 2005).
[9]A. Goldman, *Modern Ferrite Technology*, 2nd ed. (Springer, New York and NY, 2005).
[10]S. E. Lyshevski, *Nano- and Micro-Electromechanical Systems: Fundamentals of Nano- and Microengineering*, 2nd ed., Nano- and Microscience, Engineering, Technology, and Medicine Series Vol. 8 (CRC Press, Boca Raton [u.a.], 2005).